

# Icosahedral Ti-Zr-Ni: A groundstate quasicrystal?

R. G. Hennig,\* A. E. Carlsson, and K. F. Kelton

Department of Physics, Washington University, St. Louis, MO 63130, USA

C. L. Henley

Laboratory of Atomic and Solid State Physics, Cornell University, Ithaca, NY 14853, USA

(Dated: March 22, 2022)

The first complete *ab initio* zero-temperature ternary phase diagram is constructed from the calculated energies of the elemental, binary and ternary Ti-Zr-Ni phases; for this, the icosahedral *i*-TiZrNi quasicrystal phase is approximated by periodic structures of up to 123 atoms/unit cell, based on a decorated-tiling model. The approximant structures containing the 45-atom Bergman cluster were nearly degenerate, and stable against the competing binary phases. It is speculated that *i*-TiZrNi may be a ground state quasicrystal, as it is experimentally the low-temperature phase for its composition.

PACS numbers: 61.44.Br, 71.15.Nc, 81.30.Bx

Thermodynamically stable, long-range ordered quasicrystals of icosahedral symmetry are known in both of the main structural classes of quasicrystal, the Al-transition metal class (e.g. *i*-AlPdMn) and the Frank-Kasper class [1] (e.g. *i*-ZnMgY). The Ti-based quasicrystals such as *i*-TiCrSiO [2] and the thermally stable *i*-TiZrNi [3, 4, 5] fall into either respective class. They are of technical interest due to their high melting point and capacity for hydrogen absorption, but are less studied because the crystallites are small and the coherence length is only 35 nm.

In experiments on the TiZrNi alloy, the crystal structure *W*-TiZrNi is stable at high temperatures, but upon cooling it undergoes a reversible phase transition at 570°C to *i*-TiZrNi, showing that *i*-TiZrNi is lower in energy than *W*-TiZrNi [3, 6]. In fact *W*-TiZrNi is a “periodic approximant” of *i*-TiZrNi, meaning that the unit cell is identical to a fragment of the icosahedral. Long-time anneals (up to one month) at 500°C gave no indication that the quasicrystal transforms to some other phase. The situation here contrasts with the Al-transition metal class, in which the analogous crystal  $\alpha$ -AlMnSi (known as “1/1 approximant”), is lower in energy than the quasicrystal of identical composition.

In this work, we address the possibility that the *i*-TiZrNi quasicrystal (or a very large unit cell crystal of nearly identical structure) is in fact a ground state. We compute the ternary ground state phase diagram, using a database of *ab initio* total energies of 28 elemental, binary and ternary crystalline phases in the Ti-Zr-Ni alloy system. The total energy for the quasicrystal phase is determined from six different periodic approximants of *i*-TiZrNi. This calculation depends on our previously reported structure model [5], which was formulated as a decoration by atoms of the canonical cell tilings, and fitted to a combination of diffraction data and *ab initio* relaxations.

*Ti-Zr-Ni crystalline phase diagram* – To validate

the experimental findings as well as the diffraction-based structure model [5], we computed the energies of quasicrystal-like and competing structures and from this constructed the complete ground state ternary phase diagram. This is the first *ab initio* investigation of the Ti-Zr-Ni alloy system.

Our *ab initio* total energy calculations were performed with VASP [7], which is a density functional code using a plane-wave basis and ultrasoft Vanderbilt type pseudopotentials [8]. The calculations were performed using the generalized gradient approximation by Perdew and Wang [9] and a plane-wave kinetic-energy cutoff of  $E_{\text{cut}} = 302.0$  eV was chosen to ensure convergence of the energy. The pseudopotentials for Ti and Zr describe the 3p and 4p states, respectively, as semi-core states. This was found to be necessary to avoid unphysical short distances between Ti and Zr atoms. Atomic-level forces were calculated and relaxations with a conjugate gradient method were performed. The positions of the atoms, as well as the shape and volume of the unit cells, were relaxed until the total electronic energy changed by less than 1 meV. This corresponds to atomic-level forces  $F_{\text{max}} \leq 0.02$  eV/Å. The size of the k-point mesh was chosen to give the same accuracy for the energy.

The ground state phase diagram is constructed by calculating the ground state energy surface. This corresponds to determining the convex hull of the set of energy points as a function of the composition, as determined by the energy calculations for the different phases. Before investigating the whole ternary ground state phase diagram, the phase diagram for the binary phases is determined from the energy calculations. For each concentration the lowest energy structure is determined (see Table I). The convex hull of these points is then constructed by considering chemical equilibria between the different phases.

For the Ti-Ni phase diagram, we find in agreement with

TABLE I: Structures and electronic energies of the competing Ti-Zr-Ni phases: The calculated energies,  $E$ , the energy difference to the groundstate,  $\Delta E$ , and the heats of formation,  $\Delta H_f$ , are given. Wherever available, experimental values are given in parentheses [10].

Structure	$N_{\text{atoms}}$			$E$	$\Delta E$	$\Delta H_f$
	Ti	Zr	Ni	[ $\frac{\text{eV}}{\text{atom}}$ ]	[ $\frac{\text{meV}}{\text{atom}}$ ]	[ $\frac{\text{kJ}}{\text{mol}}$ ]
$\alpha$ -Ti <sup>a</sup> (A3)	2	0	0	-7.752	0	—
$\beta$ -Ti <sup>b</sup> (A2)	1	0	0	-7.647	+105	—
$\gamma$ -Ti (A1)	1	0	0	-7.704	+48	—
$\alpha$ -Zr <sup>a</sup> (A3)	0	2	0	-8.398	0	—
$\beta$ -Zr <sup>b</sup> (A2)	0	1	0	-8.351	+47	—
$\gamma$ -Zr (A1)	0	1	0	-8.344	+54	—
$\gamma$ -Ni <sup>a</sup> (A1)	0	1	0	-5.422	0	—
$\alpha$ -Ni (A3)	0	2	0	-5.410	+12	—
$\beta$ -Ni (A2)	0	1	0	-5.380	+42	—
Ti <sub>2</sub> Ni <sup>a</sup> (E9 <sub>3</sub> )	16	0	8	-7.286	0	-30 (-27)
Ti <sub>2</sub> Ni (C16)	4	0	2	-7.278	+7	-29
TiNi <sup>a</sup> (B19')	2	0	2	-7.037	+3	-43 (-34)
TiNi <sup>b</sup> (B2)	1	0	1	-6.989	+49	-39
TiNi (B <sub>f</sub> )	2	0	2	-7.040	0	-44
TiNi <sub>3</sub> <sup>a</sup> (D0 <sub>24</sub> )	4	0	12	-6.546	0	-52 (-35)
Zr <sub>2</sub> Ni <sup>a</sup> (C16)	0	4	2	-7.759	0	-34 (-37)
Zr <sub>2</sub> Ni (E9 <sub>3</sub> )	0	16	8	-7.665	+93	-25
ZrNi <sup>a</sup> (B <sub>f</sub> )	0	2	2	-7.407	0	-48 (-49)
ZrNi (B2)	0	1	1	-7.298	+109	-37
ZrNi (B19')	0	2	2	-7.407	+1	-48
Zr <sub>7</sub> Ni <sub>10</sub> <sup>a</sup> (Aba2)	0	14	20	-7.143	+5	-50 (-52)
Zr <sub>7</sub> Ni <sub>10</sub> <sup>a</sup> (Pbca)	0	28	40	-7.143	+5	-50 (-52)
ZrNi <sub>2</sub> (C15)	0	2	4	-6.864	+54	-43 (-73)
ZrNi <sub>3</sub> <sup>a</sup> (D0 <sub>19</sub> )	0	2	6	-6.674	0	-49 (-67)
Zr <sub>2</sub> Ni <sub>7</sub> <sup>a</sup> (C <sub>2</sub> /m)	0	4	14	-6.559	0	-46 (-46)
ZrNi <sub>5</sub> <sup>a</sup> (C15 <sub>b</sub> )	0	1	5	-6.287	0	-36 (-35)
$\delta$ -Ti <sub>6</sub> Zr <sub>2</sub> Ni <sub>4</sub> (E9 <sub>3</sub> )	12	4	8	-7.335	+69	-24
$\delta$ -Ti <sub>2</sub> Zr <sub>6</sub> Ni <sub>4</sub> (E9 <sub>3</sub> )	4	12	8	-7.599	+41	-29
$\lambda$ -Ti <sub>4</sub> Zr <sub>4</sub> Ni <sub>4</sub> <sup>b</sup> (C14)	4	4	4	-7.387	+135	-19
$\lambda$ -Ti <sub>6</sub> Zr <sub>4</sub> Ni <sub>2</sub> (C14)	6	4	2	-7.767	-11	-18

<sup>a</sup>Experimentally observed groundstate phase.

<sup>b</sup>Experimentally observed high-temperature phase.

the experimental phase diagram [11] the ground state phases  $\alpha$ -Ti (hcp),  $\gamma$ -Ni (fcc),  $\delta$ -Ti<sub>2</sub>Ni (E9<sub>3</sub>), and TiNi<sub>3</sub> (D0<sub>24</sub>). The TiNi martensite structure B19' [12] is found to be lower in energy than the high-temperature phase B2 and nearly degenerate with the B<sub>f</sub> structure, which to our knowledge has not been observed.

The ground state phases in the computed Zr-Ni phase diagram are, in addition to  $\alpha$ -Zr (hcp) and  $\gamma$ -Ni (fcc), the binary phases Zr<sub>2</sub>Ni (C16), ZrNi (B<sub>f</sub>), ZrNi<sub>3</sub> (D0<sub>19</sub>) and ZrNi<sub>5</sub> (C15<sub>b</sub>). This is consistent with the binary phase diagram [11]. The calculated energies for both Zr<sub>7</sub>Ni<sub>10</sub> phases, *Pbca* and *Aba2*, indicate that these phases are slightly unstable ( $\Delta E = 5$  meV/atom) and will decompose into ZrNi and ZrNi<sub>3</sub>. Our *ab initio* calculation of the binary ground state phase diagram and of the heats of formation (Table I) show excellent agreement with experiment. Furthermore, our calculated lattice param-

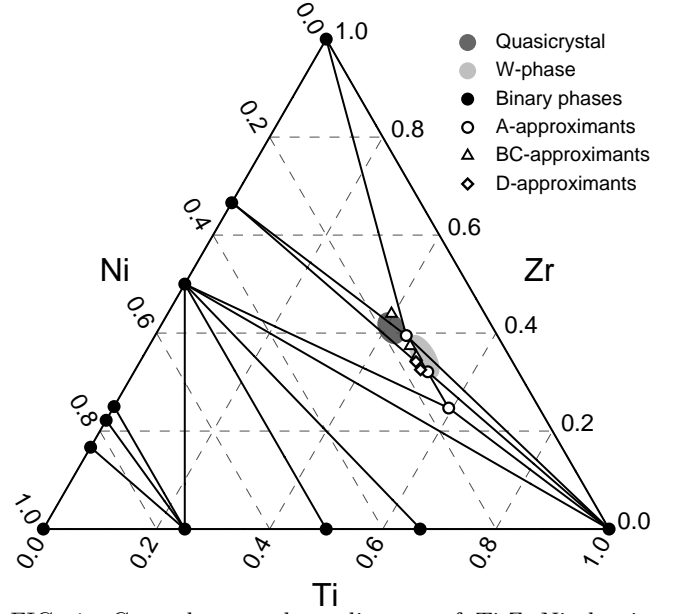


FIG. 1: Ground state phase diagram of Ti-Zr-Ni showing the creases (solid lines) of the minimum energy surface of the competing phases. Each crease represents a domain of coexistence of the two phases at that crease's end points. Each three-phase coexistence domain is a triangle bounded by creases with endpoints at the corresponding single-phase points. Shaded regions represent the experimental composition of the quasicrystal and the approximant phase.

ters (not shown here) are within 2% of the experimental values for all observed structures.

Besides the approximant phase *W*-TiZrNi and the quasicrystal *i*-TiZrNi, two ternary TiZrNi phases are observed for Ni concentrations below 50%, the hexagonal  $\lambda$ -TiZrNi phase [13, 14] and the cubic  $\delta$ -(Ti,Zr)<sub>2</sub>Ni phase [15, 16]. The  $\delta$  phase is stabilized by small amounts of oxygen and is not found in samples low in oxygen [16]; our calculations (Table I) found it to be unstable with respect to the binary phases. The atomically disordered C14 Laves phase  $\lambda$ -TiZrNi is often seen in quasicrystal samples, but is stable only at high temperatures [4]. Total energy calculations for nine deterministic ternary variants of the C14 phase showed all to be unstable against decomposition into binary phases, except for the nickel-poor  $\lambda$ -Ti<sub>6</sub>Zr<sub>4</sub>Ni<sub>2</sub>; but that in turn is computed to be less stable than the *W*-TiZrNi “approximant” structure, which has practically the same composition [14].

*Quasicrystal phase stability* – It is nontrivial to set up a computation of the quasicrystal total energy, since there is no finite unit cell. We take advantage of the description of the quasicrystal as a space-filling tiling of a few types of cell, each type containing a fixed placement (“decoration”) by atoms. A *periodic* packing of the same tiles, after decoration, forms an “approximant” structure. To estimate the total energy of the quasicrystal, we calculated that of several approximants, each made from essentially one tile type.

TABLE II: Electronic energies of periodic tiling structures approximating  $i$ -TiZrNi. Energies,  $E$ , energy differences to the groundstate,  $\Delta E$ , and to the binary phases,  $\Delta E_{\text{binary}}$ , are given.

Structure	$N_{\text{atoms}}$			$E$	$\Delta E$	$\Delta E_{\text{binary}}$
	Ti	Zr	Ni	[ $\frac{\text{eV}}{\text{atom}}$ ]	[ $\frac{\text{meV}}{\text{atom}}$ ]	[ $\frac{\text{meV}}{\text{atom}}$ ]
<i>OR</i>	3	0	1	-7.078	+324	+324
<i>PR</i>	3	2	1	-7.764	+15	+3
<i>RD</i>	8	8	3	-7.737	+110	+84
$A_6$ (1)	36	32	13	-7.827	0	-24
$A_6$ (2)	42	26	13	-7.779	0	-24
$A_6$ (3)	42	26	13	-7.731	0	-28
$B_2C_2$ (1)	42	34	15	-7.803	+4	-19
$B_2C_2$ (2)	36	40	15	-7.839	+9	-11
$B_2C_2$ (3)	44	32	15	-7.789	+4	-19
$D_2$ (1)	60	42	21	-7.773	+5	-17
$D_2$ (2)	62	40	21	-7.758	+9	-14
$i$ -TiZrNi (1)	46.0%	37.6%	16.4%	-7.806	+3	-21
$i$ -TiZrNi (2)	42.7%	40.9%	16.4%	-7.824	+6	-17

The first, simpler tiling model [1] uses the ‘‘Ammann’’ cells, a prolate (*PR*) and an oblate (*OR*) rhombohedron with edges of length 0.516 nm, as well as a composite tile called the rhombic dodecahedron (*RD*). This model’s decoration is Ni on vertices, Ti on edges, and Zr (in the role of a larger atom) in interiors. Our Ammann-cell approximants do not contain the Bergman cluster and have 4 to 19 atoms per periodic unit cell.

The second tiling model [17] uses larger ‘‘canonical cells’’ known as  $A$ ,  $B$ ,  $C$ , and  $D$ . Canonical cell structures can be viewed as a particular way to group Ammann tiles, so as to maximize the frequency of the icosahedrally symmetric 45-atom ‘‘Bergman cluster’’. The cluster centers are the canonical cell tile corners, linked by edges of 1.24 nm. This model’s atomic decoration is locally similar to the first model’s, but permits many more site types depending on the local context. In a previous paper [5], we determined the structure of  $i$ -TiZrNi by a constrained least-squares fit of this model, in which the chemical site occupations were refined using X-ray and neutron diffraction data, while the atomic positions were optimized by *ab initio* relaxations of the resulting atomic decoration for periodic tilings; two iterations of this two-step procedure gave convergence. Several sites were found to have mixed occupation, which must be chosen one way or the other in the *ab initio* calculations, producing the numbered variant decorations in Table II. The canonical-cell approximants ( $A_6$ ,  $B_2C_2$  and  $D_2$  packings) are relatively large, with 81 to 123 atoms per crystallographic unit cell [5, 17].

From the energies of the ternary approximant structures the groundstate energy surface is constructed in the same way as done for the binary phases. Table II gives the energy of formation  $\Delta E$  we found for these structures, which is defined as the energy difference to the coexisting mixture of three competing binary phases with

the same composition and the lowest possible energy, i.e. the groundstate energy surface.  $\Delta E_{\text{binary}}$  is defined in comparison to a coexisting mixture of three competing binary phases, which in our calculation are  $\alpha$ -Ti,  $\text{Zr}_2\text{Ni}$ , and (depending on the composition) either  $\alpha$ -Zr or  $\text{ZrNi}$ . Experimentally, the competing phases of the quasicrystal are  $\alpha$ -Ti/Zr,  $\text{Ti}_2\text{Ni}$ ,  $\text{Zr}_2\text{Ni}$ ,  $\lambda$ -TiZrNi (Laves phase), and the  $W$ -TiZrNi approximant phase [4].

All three periodic Ammann tiling structures are unstable against the competing binary phases. The *OR* packing is particularly unfavorable energetically. On the other hand, the *PR* packing has  $\Delta E \approx 0$ . This structure is equivalent to the cubic C15 ( $\text{MgCu}_2$ -type) Laves phase [1]; it can be obtained by replacing most of the Ni atoms in the C15  $\text{ZrNi}_2$  structure by Ti.

The quasicrystal-like periodic canonical cell tilings, on the other hand, have significantly lower energies, by up to 28 meV/atom compared to the competing binary phases and also lower in energy than the ternary C14 phase,  $\lambda$ - $\text{Ti}_6\text{Zr}_4\text{Ni}_2$ , as mentioned earlier. We found the three  $A_6$  structures to be groundstate structures and the  $B_2C_2$  as well as the  $D_2$  structures to lie slightly above the groundstate energy surface by 4 to 9 meV/atom. The  $A_6$  tiling corresponds to the experimentally observed  $W$ -TiZrNi phase (which inspired the structure model [5]). Diffraction experiments show that  $W$ -TiZrNi has Ti/Zr disorder on the two kinds of site which lie on the plane bisecting the  $\langle 100 \rangle$  axis linking two Bergman clusters [18]; therefore we investigated variant chemical occupations of these so-called ‘‘glue’’ sites. We found that all three variants give the lowest energy for their composition. In fact, the three structures form a line on the groundstate energy surface, indicating that Ti/Zr disorder on these sites costs no energy.

The next larger canonical cell tilings, the  $B_2C_2$  and the  $D_2$  tilings, do not correspond to experimentally observed phases, but are computed to be stable with respect to the binary phases. We investigated variant site occupations in both these structures [19]. Changing Zr atoms to Ti on certain sites only weakly influences the energy, whereas changing Ti atoms to Ni leads to significant increase of the energy, indicating that the quasicrystal might contain Ti/Zr disorder but not Ti/Ni disorder, in agreement with the structural refinement of  $i$ -TiZrNi of Ref. 5.

The stability of the decoration model of the three periodic canonical cell tilings is a strong indication that the decoration of a larger tiling should be practically stable. We estimated the energy of  $i$ -TiZrNi by summing the energy of each constituent tile, as found from the structures with only one kind of tile. In an infinite icosahedral canonical-cell tiling, the number ratio of tiles is  $N(A) : N(BC) : N(D) = (3[3 - \sqrt{5}] : 1 : [\sqrt{5} - 2])$ , where we adopted the ‘‘magic’’ value  $\zeta = 3(1 - 2/\sqrt{5})$ , a parameter for the frequency of  $D$  cells [17]. Taking the lowest energy tiling structures  $A_6(1)$ ,  $B_2C_2(1)$  and the  $D_2(1)$  yields for the composition of the quasicrystal

$\text{Ti}_{46.0}\text{Zr}_{37.6}\text{Ni}_{16.4}$  (1), 4% higher in Ti than the experimental composition of  $\text{Ti}_{41.5}\text{Zr}_{41.5}\text{Ni}_{17}$ . Taking the Zr rich  $B_2C_2$  (2) structure instead yields  $\text{Ti}_{42.7}\text{Zr}_{40.9}\text{Ni}_{16.4}$  (2) within 1% of the experimental composition. The energies of the periodic tilings are not enough to determine the energy of the quasicrystal since inter-tile interactions (called “tile Hamiltonian”) need to be considered too [20]. Neglecting any tile-tile interactions the two quasicrystal models are 21 and 17 meV/atom lower than the competing binary phases. Both structures, however, are slightly above the ground state energy surface by 3 and 6 meV/atom respectively [21]. This combined with the experimental results suggests that the icosahedral TiZrNi quasicrystal really may be a ground state quasicrystal.

What mechanism stabilizes the quasicrystal-like approximant structures? Ti and Zr exhibit a zero heat of mixing. Ti and Ni as well as Zr and Ni, on the other hand, show a strongly attractive interaction. Thus, it is energetically favorable for the Ni atoms to be surrounded by Ti or Zr. This is reflected in a large charge transfer from the Ti/Zr to Ni and a strong hybridization between the Ni and the Ti/Zr subbands which we observe in our calculations. This explains why in the quasicrystalline structure the Ni atoms occupy the sites along the edges of the Ammann tiles surrounded by Ti and Zr. Furthermore, since Zr is slightly larger than Ti it is no surprise that Zr occupies the more open sites of the structure.

However, the unstable small-Ammann-tiling approximants *PR*, *OR*, and *RD* have virtually the same *local* atomic structure as the canonical-cell approximants  $A_6$ ,  $B_2C_2$ , and  $D_2$ . The main difference is that complete Bergman clusters are absent in the small Ammann approximants, but dense in the canonical cell approximants (where they contain  $\sim 1/2$  of the atoms); we conjecture that this is responsible for the energy difference.

*Conclusion* – The first systematic investigation of the energies of structures of the binary Ti-Ni and Zr-Ni phase diagrams was presented and it was shown that *ab initio* calculations for these systems yield excellent agreement for the ground state phases with experiments. The phase transition between the *W* phase and the quasicrystal observed experimentally as well as the long-time annealing experiments demonstrate that the quasicrystal is a stable low temperature phase. The *ab initio* energies of the nickel-poor Ti-Zr-Ni ternary crystalline phases showed that only the large-cell “quasicrystal approximants” containing complete Bergman clusters were stable against decomposition into the binary phases. This demonstrates that the *i*-TiZrNi phase, the *W*-TiZrNi phase, or a similar large-cell approximant is the groundstate of the system. The calculations (Table II) imply a *total* energy difference favoring *W*-TiZrNi by the order of 100 meV per *tile*. The experimental situation indicates that *i*-TiZrNi is stabilized by energy. Conceivably the quasicrystal – or large approximants that mix different canonical cell types – could be stabilized by the cell-cell interaction

energies, which were hitherto neglected. Energy calculations on those larger approximants would permit the extraction of the tile Hamiltonian, which is needed to decide whether the quasicrystal is a ground state, and to address its long-range structure.

The work at Washington University was supported by the National Science Foundation (NSF) under grants DMR 97-05202 and DMR 00-72787. C.L.H. was supported by D.O.E. grant DE-FG02-89ER-45405. R.G.H. was partially supported by NSF grant DMR-0080766 and by DOE grant DE-FG02-99ER45795.

---

\* Current address: Ohio State University, Department of Physics, Columbus, OH 43210, USA.

- [1] C. L. Henley and V. Elser, *Phil. Mag. B* **53**, L59 (1986).
- [2] R. G. Hennig and H. Teichler, *Phil. Mag. A* **76**, 1053 (1997).
- [3] K. F. Kelton, W. J. Kim, and R. M. Stroud, *Appl. Phys. Lett.* **70** (1997).
- [4] J. P. Davis, E. H. Majzoub, J. M. Simmons, and K. F. Kelton, *Mat. Sci. Eng. A* **294-296**, 104 (2000).
- [5] R. G. Hennig, K. F. Kelton, A. E. Carlsson, and C. L. Henley, Submitted to *Phys. Rev. B*, cond-mat/0202536 (2001).
- [6] S. Yi and D. H. Kim, *J. Mat. Res.* **15** (2000).
- [7] G. Kresse and J. Hafner, *Phys. Rev. B* **47**, RC558 (1993), G. Kresse and J. Furthmüller, *Comp. Mat. Sci.* **6**, 15 (1996), *Phys. Rev. B* **54**, 11169 (1996).
- [8] D. Vanderbilt, *Phys. Rev. B* **41**, 7892 (1990), G. Kresse and J. Hafner, *J. Phys.: Condens. Matter* **6**, 8245 (1994).
- [9] J. P. Perdew and Y. Wang, *Phys. Rev. B* **45**, 13244 (1992).
- [10] F. R. de Boer, R. Boom, W. C. M. Mattens, A. R. Miedema, and A. K. Niessen, *Cohesion in Metals: Transition Metal Alloys* (Amsterdam: North-Holland, 1988).
- [11] T. B. Massalski, J. L. Murray, L. H. Bennett, and H. Baker, *Binary Alloy Phase Diagrams* (Metals Park, Ohio: American Society for Metals, 1986).
- [12] M. J. Marcinkowski, A. S. Sastri, and D. Koskimaki, *Phil. Mag.* **18**, 945 (1968).
- [13] V. V. Molokanov, V. N. Chebotnikov, and Y. K. Kovneristyi, *Inorganic Materials* **25**, 46 (1989).
- [14] E. H. Majzoub, R. G. Hennig, and K. F. Kelton, submitted to *Phil. Mag. A* (2001).
- [15] G. A. Yurko, J. W. Barton, and F. G. Parr, *Acta Cryst.* **12**, 909 (1959).
- [16] R. Mackay, G. J. Miller, and H. F. Franzen, *J. Alloys Compd.* **204**, 109 (1994).
- [17] C. L. Henley, *Phys. Rev. B* **43**, 993 (1991).
- [18] R. G. Hennig, E. H. Majzoub, A. E. Carlsson, K. F. Kelton, C. L. Henley, W. B. Yelon, and S. Misure, *Mat. Sci. Eng. A* **294-296**, 361 (2000).
- [19] R. G. Hennig, Ph.D. thesis, Washington University in St. Louis (2000).
- [20] M. Mihalkovič, W. J. Zhu, C. L. Henley, and R. Phillips, *Phys. Rev. B* **53**, 9021 (1996).
- [21] The (small) energy differences here are roughly half those calculated for model *i*-AlMn quasicrystals using *ab-initio* based pair potentials (See Ref. 20, Fig. 5).